Online Submissions: wjg.wjgnet.com
wjg@wjgnet.com
doi:10.3748/wjg.15.2139

World J Gastroenterol 2009 May 7; 15(17): 2139-2144
World Journal of Gastroenterology ISSN 1007-9327

Evaluation of a rabbit rectal VX2 carcinoma model using computed tomography and magnetic resonance imaging

Xin-Mei Liang, Guang-Yu Tang, Ying-Sheng Cheng, Bi Zhou

Xin-Mei Liang, Bi Zhou, Department of Radiology, the Sixth People's Hospital of Shanghai Jiaotong University; Institute of Medical Imaging of Shanghai Jiaotong University, No. 600, Yishan Road, Shanghai 200233, China
Guang-Yu Tang, Ying-Sheng Cheng, Department of Radiology, the Tenth People's Hospital of Shanghai Tongji University, No. 301, Yanchang Middle Road, Shanghai 200072, China
Author contributions: Liang XM and Cheng YS contributed equally to this work; Liang XM and Cheng YS designed the research; Liang XM and Zhou B performed the research; Liang XM analyzed the data and wrote the paper; Tang GY and Cheng YS revised the paper.
Correspondence to: Dr. Ying-Sheng Cheng, Professor, Department of Radiology, the Tenth People's Hospital of Shanghai Tongji University, No. 301, Yanchang Middle Road, Shanghai 200072, China. cjr.chengysh@vip.163.com
Telephone: +86-21-66301136 Fax: +86-21-66303983
Received: February 6, 2009 Revised: March 8, 2009
Accepted: March 15, 2009
Published online: May 7, 2009

Abstract

AIM: To establish a rabbit rectal VX2 carcinoma model for the study of rectal carcinoma.

METHODS: A suspension of VX2 cells was injected into the rectum wall under the guidance of X-ray fluoroscopy. Computed tomography (CT) and magnetic resonance imaging (MRI) were used to observe tumor growth and metastasis at different phases. Pathological changes and spontaneous survival time of the rabbits were recorded.

RESULTS: Two weeks after VX2 cell implantation, the tumor diameter ranged 4.1-5.8 mm and the success implantation rate was 81.8%. CT scanning showed low-density foci of the tumor in the rectum wall, while enhanced CT scanning demonstrated asymmetrical intensification in tumor foci. MRI scanning showed a low signal of the tumor on T_1-weighted imaging and a high signal of the tumor on T_2-weighted imaging. Both types of signals were intensified with enhanced MRI. Metastases to the liver and lung could be observed 6 wk after VX2 cell implantation, and a large area of necrosis appeared in the primary tumor. The spontaneous survival time of rabbits with cachexia and multiple organ failure was about 7 wk after VX2 cell implantation.

CONCLUSION: The rabbit rectal VX2 carcinoma model we established has a high stability, and can be used in the study of rectal carcinoma.

Key words: Rectal carcinoma; Animal model; Rabbit; VX2; Computed tomography; Magnetic resonance imaging

Peer reviewers: Yik-Hong Ho, Professor, Department of Surgery, School of Medicine, James Cook University, Townsville 4811, Australia; Dr. Tommaso Cioppa, Department of General and Oncological Surgery, "San Giuseppe" Hospital, Viale Boccaccio, 50053, Empoli (Florence), Italy

Liang XM, Tang GY, Cheng YS, Zhou B. Evaluation of a rabbit rectal VX2 carcinoma model using computed tomography and magnetic resonance imaging. *World J Gastroenterol* 2009; 15(17): 2139-2144 Available from: URL: http://www.wjgnet.com/1007-9327/15/2139.asp DOI: http://dx.doi.org/10.3748/wjg.15.2139

INTRODUCTION

Rectal carcinoma is a common malignant tumor of the gastrointestinal tract. Imaging examination plays an important role in its identification, diagnosis, preoperative staging, treatment decision, and postoperative assessment[1-3]. Currently, experimental animal models of rectal carcinoma are often induced by chemical carcinogens[4-6]. This kind of methods requires lots of time and individual variations can be very large. In this study, a rabbit rectal carcinoma model was established and evaluated, which can be monitored dynamically by computed tomography (CT) and magnetic resonance imaging (MRI) and used in diagnosing and staging rectal carcinoma.

MATERIALS AND METHODS

Experimental animals

Twenty-two (4-5 mo old) New Zealand white rabbits, weighing 2.4-2.9 kg, were used in this study, and the breeding rabbits were donated by Professor Bin Hu,

Department of Ultrasound, Sixth People's Hospital of Shanghai Jiaotong University, China.

Preparation for surgery

Experimental rabbits were lavaged 24 h prior to surgery. Mannitol (20%) was prepared with warm water at a ratio of 1:1 and the lavage dose was approximately 250 mL per rabbit. Lavaged rabbits were fasted with free access to water prior to surgery. VX2 tumor cells were grown in the hind leg muscle of rabbits and harvested for the preparation of suspended tumor cells at a concentration of 1-2 × 10^7/mL.

Establishment of rectal carcinoma model

Experimental rabbits were anesthetized with 30 mg/kg pentobarbital sodium *via* the ear vein. Rabbits were placed at a dorsal position with their legs fixed. A 7-cm long sterilized plastic hollow pipe, 7 mm in diameter, was inserted into the anus to brace the rectal cavity. A 22G transfixion pin was injected into approximately 4-5 cm of the rectal wall around the anus. A contrast medium (0.2 mL, Ultravist 300) was injected with its distribution monitored by X-ray fluoroscopy. If its border was ill-defined and dispersed, the needle point would be in a gap region between the outside of the organ and the rectal wall. Then, the puncture needle was reinserted into the rectal wall until the border of contrast medium became sharply margined. At this point, 0.2 mL of suspended VX2 cells was injected, then 0.1-0.2 mL of normal sodium was injected to fully rinse all the VX2 cells into the rectal wall. After 5 min, the needle was withdrawn slowly. The rabbits were allowed to have normal food following recovery from anesthesia.

CT and MRI scanning of tissue sections

Rabbits were anesthetized with 30 mg/kg pentobarbital sodium before CT and MRI scanning of tissue sections at 2-, 3-, 4-, 5- and 6-wk intervals after VX2 cell implantation. CT scanning was performed using a GE LIGHT SPEED VCT 64 CT set with the following parameters: 80 kV, 100 mA, 14-16 cm in field of view (FOV), 512*512 matrix, 1.25 mm section thickness, and 1.25 mm section interval. A contrast medium (Ultravist 300) was injected at 0.5 mL/s and 1.5-2.0 mL/kg. Arterial phase scanning was started 15 s after contrast medium injection and after 30 s during the portal venous phase. The image was processed at the ADW4.0 workstation. MRI scanning was performed by a Philips Achieva 3.0 imager, with the rabbit placed at a supine position in a phased-array articular genu coil. MRI sequences included the pre-contrast T_1W-TSE, gadolinium-enhanced T_1W-TSE, and T_2W-TSE sequences in the axial plane (TR-2727 ms, TE-100 ms, 2.0 mm section thickness 2.0 mm, and section interval 0.8 mm), T_2_TSE_SPAIR sequence in the axial plane (TR-4341 ms, TE-62 ms, section thickness 2.0 mm, and section interval 0.2 mm), and PD_SPAIR sequence in the coronal planes (TR-4710 ms, TE-30 ms, section thickness 2.0 mm, and 0.2 mm section interval 0.2 mm). The contrast medium (Magnevist) was injected at 0.5 mL/s and 1.5-2.0 mL/kg. Enhancement scanning was started 20 s after contrast medium injection, and the image was processed at a View Forum R5.1 V1L1 workstation.

Measurement of tumor volume

Gross tumor volume (V) was measured following the equation: $V = 0.5 (a \times b^2)$, where a represents the maximum tumor diameter, and b represents the minimum tumor diameter. Tumor growth rate (TGR) was calculated following the equation: $TGR = (V_2 - V_1)/V_1 \times 100\%$, where V_1 represents the gross tumor volume measured at an earlier time point and V_2 represents the gross tumor volume measured at a later time point.

Histopathological changes in rabbit rectal VX2 carcinoma model

Three rabbits were sacrificed after each CT and MRI scanning at 2-6 wk intervals after VX2 cell implantation for observation of pathological changes in the rectal VX2 carcinoma model. Autopsies were also performed after spontaneous death of the rabbits. Tumor location, size, activity, circumscription, and metastasis were observed grossly. The rectum-implanted tumor and the major organs involved were fixed in formalin and embedded in paraffin. Tumor tissue was cut into sections, which were stained with hematoxylin-eosin (H&E), and evaluated under a light microscope.

Statistical analysis

Data were presented as mean ± SD. Gross tumor volumes at an earlier and later time point were compared by Student's *t* test. Statistical analyses were performed using SPSS 11.0 software. $P < 0.05$ was considered statistically significant.

RESULTS

Twenty-two New Zealand white rabbits were used to establish the model. Eighteen of them developed primary tumors with a success rate of 81.8%.

CT detection

Tumor implanted in the rectal wall of each rabbit could be detected by CT scanning 2 wk after VX2 cell implantation. The appearance of rectal enteric cavity at this time point was still normal without obvious stricture. However, part of the rectal wall exhibited irregularly intensified armillary after enhancement (Figure 1A). The gross tumor volume was increased 3 wk after VX2 cell implantation, and appeared as a small lump with low density or isodensity on CT images. The boundary between the tumor and normal rectal wall could not be clearly distinguished. However, the rectal enteric cavity became elliptical with stricture, allowing the tumor margin to be distinguished from its surrounding tissue (Figure 1B). After 4 wk, the gross tumor volume was increased, the rectal wall was thickened, and the rectal enteric cavity became flatter, with increased stricture.

Table 1 Gross tumor volume and TGR after tumor implantation

Time after implantation	a (mm)	b (mm)	V (mm^3)	TGR (%)
2 wk	5.029 ± 0.544	4.129 ± 0.475	46.180 ± 14.583	-
3 wk	16.783 ± 1.387	9.942 ± 1.326	848.239 ± 270.715	1736.8
4 wk	19.419 ± 1.150	15.800 ± 1.255	2443.569 ± 480.966	185.7
5 wk	24.763 ± 1.762	22.163 ± 1.388	6163.157 ± 1181.274	159.3

Tumor volume (V) = 0.5 ($a \times b^2$), where a and b represent the maximum and minimum tumor diameters, respectively; TGR = (V_2 - V_1)/V_1 × 100%, where V_1 represents the gross tumor volume measured at an earlier time point and V_2 represents the gross tumor volume measured at a later time point.

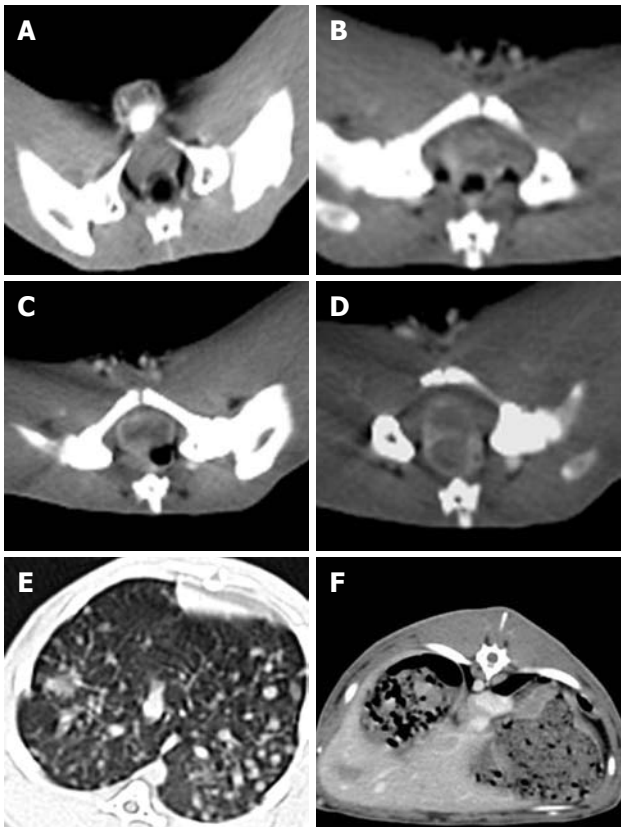

Figure 1 CT enhancement scanning images of rectal wall 2(A), 3(B), 4(C), and 5(D) wk after VX2 cell implantation in the experimental rabbits, and images of metastatic nodes detected in the lung (E) and liver (F), respectively.

Necrosis could be detected in the middle of the tumor, and the surrounding tissue was involved at different degrees. CT scanning showed that the tumor appeared to have an intensified, solid marginal zone and a central region with low density but without intensification. In contrast, the surrounding tissue was intensified as the tumor (Figure 1C). CT scanning revealed significant stricture of the tumor, which was fixed to the pelvic wall and rectal enteric cavity 5 wk after VX2 cell implantation (Figure 1D). After 6 wk, the rectal enteric cavity was almost compressed to the point of closure and metastatic nodes were detected in the lung (Figure 1E) and liver (Figure 1F), as in the seroperitoneum. The metastatic nodes appeared in the lung earlier and much more obviously than in the liver, since the blood supply in the lower part of rectum returns to the inferior vena cava but not to the hepatic portal vein.

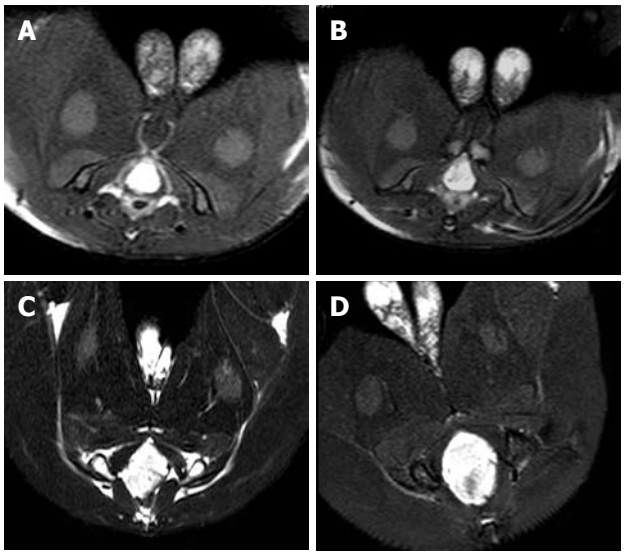

Figure 2 MRI of T2-TSE-SPAIR 2(A), 3(B), 4(C), and 5(D) wk after VX2 cell implantation in the experimental rabbits.

MRI detection

MRI showed that the signal of VX2 tumor was low on T_1-weighted imaging (T_1WI), resulting in the detection of an indistinct boundary, and high on T_2-weighted imaging (T_2WI), allowing clear visualization of the boundary. In addition, the signal of VX2 tumor in PD sequence was higher than that on T_1WI. Tumor boundary could be distinguished from its surrounding tissue after enhancement. Necrosis with low signals, but without intensification after enhancement, could be detected in the middle of the primary tumor 4 wk after VX2 cell implantation. MRI and CT demonstrated similar growth and metastasis of the tumor. However, MRI identified more precisely the tumor boundary, size and infiltration, and infection foci than CT scanning. MRI of the tumor at 2-, 3-, 4-, and 5-wk intervals after VX2 cell implantation are shown in Figure 2. The gross tumor volume (V) and the TGR at these time points were also calculated (Table 1). The TGR at each time point was quite different ($P < 0.0001$), but the fastest growth of tumor was observed 3 wk after VX2 cell implantation.

Histopathological changes

Macroscopic image of the resected tumor appeared as a single node with an obscure boundary and affluent vascellum (Figure 3A and B). Metastasis

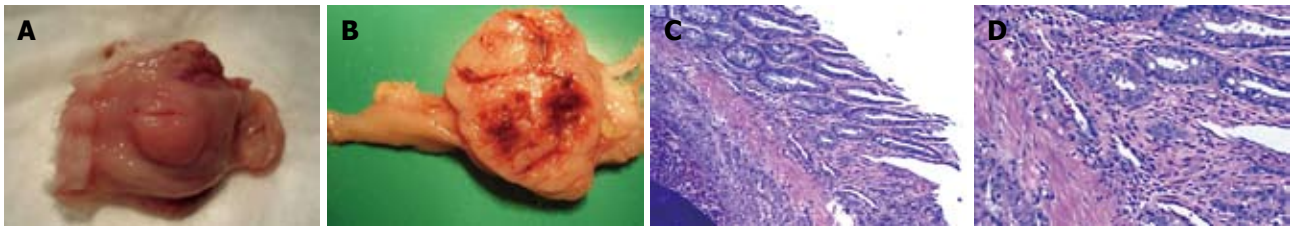

Figure 3 Characteristics of isolated rectal carcinoma specimens (A, B) and light microscope images of HE stained tissue sections (C, × 40; D, × 100).

outside the rectal wall was not detected until 4 wk after VX2 cell implantation. The rectal wall was thickened due to different degrees of enteric cavity stricture. No enterectasis or rectum obstruction was observed. Necrosis appeared in the middle of the tumor 4 wk after VX2 cell implantation, with enteric cavity stricture and enterectasis, as well as metastasis outside the rectal wall in the pelvic cavity. Metastases to the lung and liver, and seroperitoneum and rectum obstruction were detected 6 wk after VX2 cell implantation. However, the metastasis in the liver was not as obvious as that in the lung, and sometimes it was not detectable, because the metastasis in the liver was not sufficiently large to be visualized. The experimental rabbits developed cachexia and multiple organ failure, and died spontaneously about 7 wk after VX2 cell implantation.

Tumor tissue sections were stained with H&E and evaluated under a light microscope. Infiltrating tumor cells were visible and the interstitial tissue boundary was not distinct. Minimal connective tissue was observed, and dispersed tumor cells were found with separation of fibers. Fresh capillaries were abundant (Figure 3C), consistent with the large, irregular tumor volume. Cytoplasm of the tumor cells was abundant, and pale red in color. There was an abnormal number of mitotic nuclei. Hypertrophic nuclei were also found, varying in shape, size, and color (Figure 3D). Two weeks after VX2 cell implantation, the tumor grew in the rectal wall with no involvement of its peripheral tissue. However, by 3 wk after VX2 cell implantation, the tumor grew through the rectal wall with the mesorectal fascia tissue involved 4 wk after VX2 cell implantation.

DISCUSSION

Since lymph in the gastrointestinal tract is very rich, the survival rate of heterogeneic tumor tissue transplanted to the intestine wall of experimental animals is practically zero. Because of this, smaller animal models are often used in the study of rectal carcinoma. Experimental animal models can be established by repeated injection of chemical carcinogens into the abdominal cavity of animals, or repeated lavaging of the intestinal tract. However, these methods are time consuming and their success rate is low. Furthermore, these small animal models cannot contribute to the diagnosis of rectal carcinoma.

VX2 cells can be implanted into rabbits where they can grow. It has been shown that this cell line, implanted into the muscle, kidney, liver, lung, pleura, ossature, and mammary gland of rabbits, can produce an *in situ* tumor model that mimics the human condition[7-12]. The implantation techniques for VX2 cells include implanting a small lump of VX2 tumor tissue and injecting a suspension of VX2 cells directly or under the guidance of B-mode ultrasound or CT. Wang *et al*[13] demonstrated that laparotomy could be used to establish a rabbit model of rectal VX2 carcinoma, with a success rate of 60%. Considering the substantial damage caused by laparotomy, we established the rabbit model of rectal VX2 carcinoma by injecting a suspension of VX2 cells into the rectal wall through the skin of the anorectum under the guidance of X-ray fluoroscopy. CT or MRI showed the implanted tumor in the rectal wall 2 wk after VX2 cell implantation. The involved tissue around the rectum was observed and metastases to the lung and liver were detectable 4 and 6 wk, respectively, after VX2 cell implantation. The success rate of this method was 81.8%.

This rabbit rectal VX2 carcinoma model was evaluated by CT scanning, MRI, and histopathology.

CT has many advantages in monitoring rectal tumor by displaying its location, size, shape, peripheral tissue and lymph node involvement[14,15]. Recently, with the update of CT instruments and CT imaging techniques, the sensitivity and specificity of CT in detection of tumors have been greatly improved. Multi-section CT (MSCT) is more advantageous than ordinary CT, by reducing the shadow of motion and displaying dynamic enhancement effects[16-18]. Furthermore, CT plays an important role in preoperative staging of rectal carcinoma, especially in detecting metastasis in the lung and liver[19]. CT scanning has been recommended to patients with colorectal cancer[20-22]. In this study, MSCT showed the growth of tumor and its surrounding tissue, as well as distant organ metastasis, suggesting that CT scanning is an ideal method for monitoring VX2 rectal carcinoma.

Since the location of the rectum is relatively fixed, tumor tissue can be observed by contrast with the peripheral fat, and is seldom affected by the shadows that result from respiration. MRI is a good imaging technique for detection of rectal tumor and can show the layers of the rectal wall, including the mucosa with a low-intensity signal, submucosa with a high-intensity signal, muscularis propria with a weak-intensity signal, perirectal fat with a high-intensity signal, and mesorectal fascia with a low-intensity signal. T_1WI can be used to evaluate fatty infiltration around the rectum, while T_2WI can display the infiltration depth in the rectal wall

and the relation between inherent muscle layers and mesorectal fascia. The most significant advantage of MRI in rectal carcinoma staging is its ability to describe the correlation between tumor and mesorectal fascia[23-25]. MRI can determine the circumferential resection margin (CRM)[26]. Induction of 3.0T magnetic resonance and improvement in phased-array coils make MRI display the CRM much more precisely[27,28]. Its accuracy for the prediction of CRM is consistent with histopathological assessment of specimens after surgery[29-32]. It has also been reported that MRI can predict the infiltration depth of rectal tumor in the range of 0.5 mm[33], which is consistent with histopathology results. MRI is more sensitive in detecting early stage tumor growth than CT, especially in measuring the tumor size. In addition, MRI can display metastasis of tumor to lymph nodes.

This animal model is easy to establish, reproducible, and induces minimal damage to experimental animals. In addition, the tumor growth time is short. The growth and metastasis of rectal VX2 carcinoma in rabbits are similar to those in humans. Therefore, it can be used in the study of rectal carcinoma.

COMMENTS

Background

Currently, experimental animal models of rectal carcinoma are often induced by chemical carcinogens, which is time consuming. It has been shown that implantation of VX2 cells into the muscle, kidney, liver, lung, pleural, ossature, and mammary gland of rabbits can produce an *in situ* tumor model that mimics the human condition.

Research frontiers

The implantation techniques for VX2 cells include implanting a small lump of VX2 tumor tissue and injecting a suspension of VX2 cells directly, or under the guidance of B-mode ultrasound and computed tomography.

Innovations and breakthroughs

It is feasible to establish a rabbit rectal VX2 carcinoma model by injecting a suspension of VX2 cells into the rectum wall under the guidance of X-ray fluoroscopy. This model is similar to human rectal carcinoma models in terms of tumor pathology, development, and metastasis.

Applications

This rabbit rectal VX2 carcinoma model can be used in examination, staging and diagnosis of rectal carcinoma.

Terminology

VX2 cell strain, a squamous carcinoma strain induced by Shope virus, can be implanted in rabbits.

Peer review

The animal model presents many analogies to human rectal carcinoma in terms of pathological findings and tumor development.

REFERENCES

1 **Low G**, Tho LM, Leen E, Wiebe E, Kakumanu S, McDonald AC, Poon FW. The role of imaging in the pre-operative staging and post-operative follow-up of rectal cancer. *Surgeon* 2008; **6**: 222-231

2 **Adeyemo D**, Hutchinson R. Preoperative staging of rectal cancer: pelvic MRI plus abdomen and pelvic CT. Does extrahepatic abdomen imaging matter? A case for routine thoracic CT. *Colorectal Dis* 2009; **11**: 259-263

3 **Iafrate F**, Laghi A, Paolantonio P, Rengo M, Mercantini P, Ferri M, Ziparo V, Passariello R. Preoperative staging of rectal cancer with MR Imaging: correlation with surgical and histopathologic findings. *Radiographics* 2006; **26**: 701-714

4 **Hinoi T**, Akyol A, Theisen BK, Ferguson DO, Greenson JK, Williams BO, Cho KR, Fearon ER. Mouse model of colonic adenoma-carcinoma progression based on somatic Apc inactivation. *Cancer Res* 2007; **67**: 9721-9730

5 **Colnot S**, Niwa-Kawakita M, Hamard G, Godard C, Le Plenier S, Houbron C, Romagnolo B, Berrebi D, Giovannini M, Perret C. Colorectal cancers in a new mouse model of familial adenomatous polyposis: influence of genetic and environmental modifiers. *Lab Invest* 2004; **84**: 1619-1630

6 **Mori F**, Piro FR, Della Rocca C, Mesiti G, Giampaoli S, Silvestre G, Lazzaro D. Survivin and Cyclooxygenase-2 are co-expressed in human and mouse colon carcinoma and in terminally differentiated colonocytes. *Histol Histopathol* 2007; **22**: 61-77

7 **Virmani S**, Harris KR, Szolc-Kowalska B, Paunesku T, Woloschak GE, Lee FT, Lewandowski RJ, Sato KT, Ryu RK, Salem R, Larson AC, Omary RA. Comparison of two different methods for inoculating VX2 tumors in rabbit livers and hind limbs. *J Vasc Interv Radiol* 2008; **19**: 931-936

8 **Choi JA**, Kang EY, Kim HK, Song IC, Kim YI, Kang HS. Evolution of VX2 carcinoma in rabbit tibia: magnetic resonance imaging with pathologic correlation. *Clin Imaging* 2008; **32**: 128-135

9 **Chen J**, Yao Q, Li D, Zhang B, Li L, Wang L. Chemotherapy targeting regional lymphatic tissues to treat rabbits bearing VX2 tumor in the mammary glands. *Cancer Biol Ther* 2008; **7**: 721-725

10 **Hu HY**, Li Q, Han ZG, Kang DQ. [Efficacy and safety of percutaneous microwave coagulation therapy for experimental vx2 lung cancer in rabbits] *Aizheng* 2007; **26**: 942-946

11 **Kreuter KA**, El-Abbadi N, Shbeeb A, Tseng L, Mahon SB, Narula N, Burney T, Colt H, Brenner M. Development of a rabbit pleural cancer model by using VX2 tumors. *Comp Med* 2008; **58**: 287-293

12 **Lee JM**, Kim SW, Chung GH, Lee SY, Han YM, Kim CS. Open radio-frequency thermal ablation of renal VX2 tumors in a rabbit model using a cooled-tip electrode: feasibility, safety, and effectiveness. *Eur Radiol* 2003; **13**: 1324-1332

13 **Wang XD**, Zhang JX, Shang D, Zhen QC. Establishment and biological characterization of rectal cancer by transplant VX2 in a rabbit. *Zhong Liu* 2006; **26**: 788-789

14 **Yano H**, Saito Y, Takeshita E, Miyake O, Ishizuka N. Prediction of lateral pelvic node involvement in low rectal cancer by conventional computed tomography. *Br J Surg* 2007; **94**: 1014-1019

15 **Pomerri F**, Maretto I, Pucciarelli S, Rugge M, Burzi S, Zandonà M, Ambrosi A, Urso E, Muzzio PC, Nitti D. Prediction of rectal lymph node metastasis by pelvic computed tomography measurement. *Eur J Surg Oncol* 2009; **35**: 168-173

16 **Cui CY**, Li L, Liu LZ. [Value of multislice spiral CT in preoperative staging of rectal carcinoma] *Aizheng* 2008; **27**: 196-200

17 **Kanamoto T**, Matsuki M, Okuda J, Inada Y, Tatsugami F, Tanikake M, Yoshikawa S, Narabayashi I, Kawasaki H, Tanaka K, Yamamoto T, Tanigawa N, Egashira Y, Shibayama Y. Preoperative evaluation of local invasion and metastatic lymph nodes of colorectal cancer and mesenteric vascular variations using multidetector-row computed tomography before laparoscopic surgery. *J Comput Assist Tomogr* 2007; **31**: 831-839

18 **Burton S**, Brown G, Bees N, Norman A, Biedrzycki O, Arnaout A, Abulafi AM, Swift RI. Accuracy of CT prediction of poor prognostic features in colonic cancer. *Br J Radiol* 2008; **81**: 10-19

19 **Kirke R**, Rajesh A, Verma R, Bankart MJ. Rectal cancer: incidence of pulmonary metastases on thoracic CT and correlation with T staging. *J Comput Assist Tomogr* 2007; **31**: 569-571

20 **Van Cutsem EJ**, Kataja VV. ESMO Minimum Clinical

Recommendations for diagnosis, adjuvant treatment and follow-up of colon cancer. *Ann Oncol* 2005; **16** Suppl 1: i16-i17
21 **Van Cutsem EJ**, Oliveira J, Kataja VV. ESMO Minimum Clinical Recommendations for diagnosis, treatment and follow-up of advanced colorectal cancer. *Ann Oncol* 2005; **16** Suppl 1: i18-i19
22 **Tveit KM**, Kataja VV. ESMO Minimum Clinical Recommendations for diagnosis, treatment and follow-up of rectal cancer. *Ann Oncol* 2005; **16** Suppl 1: i20-i21
23 **Beets-Tan RG**, Beets GL. Rectal cancer: review with emphasis on MR imaging. *Radiology* 2004; **232**: 335-346
24 **Brown G**. Thin section MRI in multidisciplinary pre-operative decision making for patients with rectal cancer. *Br J Radiol* 2005; **78** Spec No 2: S117-S127
25 **McMahon CJ**, Smith MP. Magnetic resonance imaging in locoregional staging of rectal adenocarcinoma. *Semin Ultrasound CT MR* 2008; **29**: 433-453
26 **Brown G**, Radcliffe AG, Newcombe RG, Dallimore NS, Bourne MW, Williams GT. Preoperative assessment of prognostic factors in rectal cancer using high-resolution magnetic resonance imaging. *Br J Surg* 2003; **90**: 355-364
27 **Kim SH**, Lee JM, Lee MW, Kim GH, Han JK, Choi BI. Diagnostic accuracy of 3.0-Tesla rectal magnetic resonance imaging in preoperative local staging of primary rectal cancer. *Invest Radiol* 2008; **43**: 587-593
28 **Kim CK**, Kim SH, Chun HK, Lee WY, Yun SH, Song SY, Choi D, Lim HK, Kim MJ, Lee J, Lee SJ. Preoperative staging of rectal cancer: accuracy of 3-Tesla magnetic resonance imaging. *Eur Radiol* 2006; **16**: 972-980
29 **Bianchi PP**, Ceriani C, Rottoli M, Torzilli G, Pompili G, Malesci A, Ferraroni M, Montorsi M. Endoscopic ultrasonography and magnetic resonance in preoperative staging of rectal cancer: comparison with histologic findings. *J Gastrointest Surg* 2005; **9**: 1222-1227; discussion 1227-1228
30 **Wieder HA**, Rosenberg R, Lordick F, Geinitz H, Beer A, Becker K, Woertler K, Dobritz M, Siewert JR, Rummeny EJ, Stollfuss JC. Rectal cancer: MR imaging before neoadjuvant chemotherapy and radiation therapy for prediction of tumor-free circumferential resection margins and long-term survival. *Radiology* 2007; **243**: 744-751
31 **Smith NJ**, Shihab O, Arnaout A, Swift RI, Brown G. MRI for detection of extramural vascular invasion in rectal cancer. *AJR Am J Roentgenol* 2008; **191**: 1517-1522
32 **Smith NJ**, Barbachano Y, Norman AR, Swift RI, Abulafi AM, Brown G. Prognostic significance of magnetic resonance imaging-detected extramural vascular invasion in rectal cancer. *Br J Surg* 2008; **95**: 229-236
33 **MERCURY Study Group**. Extramural depth of tumor invasion at thin-section MR in patients with rectal cancer: results of the MERCURY study. *Radiology* 2007; **243**: 132-139

S- Editor Tian L **L- Editor** Wang XL **E- Editor** Zheng XM